Triggerable multivalent glyconanoparticles for probing carbohydrate-carbohydrate interactions

*Sangho Won,[a] Steven Hindmarsh[c] and Matthew I. Gibson[a,b]**

[a] Department of Chemistry, University of Warwick, Gibbet Hill Road, Coventry, CV4 7AL, UK; [b] Warwick Medical School, University of Warwick, Gibbet Hill Road, Coventry, CV4 7AL, UK; [c] Department of Physics, University of Warwick, Gibbet Hill Road, Coventry CV4 7AL, UK

ABSTRACT: Carbohydrate-carbohydrate interactions are proposed to be biologically significant but have lower affinities than the well-studied carbohydrate-protein interactions. Here we introduce multivalent glyco-nanostructures where the surface-expression of lactose can be triggered by an external stimulus, and a gold nanoparticle core enables colorimetric signal outputs to probe binding. Macromolecular engineering of a responsive polymer 'gate' enables the lactose moieties to be presented only when an external stimulus is present, mimicking of how Nature uses enzymes to dynamically regulate glycan expression. Two different carbohydrate-carbohydrate interactions are investigated using this tool.

Cells from across all kingdoms of life are coated with glycans (polysaccharides, glycolipids, glycoproteins) which provide internal and external cues for recognition, disease state, signal transduction and more.[1] The protein 'readers' of glycans are termed lectins, which engage in relatively weak interactions with individual glycans with mM affinity.[2,3] To overcome this, glycans are presented on cells in a multivalent format, enabling a non-linear increase in binding affinity (often <nM), termed the 'cluster glycoside effect'[4] leading to dramatic increases in affinity.[4] Inspired by this, synthetic materials bearing multiple carbohydrates have been developed which also have high affinity[5] and can compete for native ligands in anti-adhesion therapy,[6–8] or as biosensors.[9,10]

Whilst carbohydrate-lectin interactions have been extensively studied and a huge variety of tools exist to probe them, carbohydrate-carbohydrate interactions (CCI) where the sugars directly engage with each other are much less studied and their biological importance is not entirely clear.[11] Glycosphingolipid CCI's have been implicated in the initial stages of cell-cell recognition[12] and the aggregation of marine sponges is linked to sulfated glycan CCI's.[13,14] The affinity of CCIs is extremely weak, even compared to carbohydrate-lectin interactions (~mM) and require divalent metal ions to bridge the glycans; multivalent presentation is essential to enable significant interaction forces to be generated.[11,15,16] Murthy et al have synthesized lactose-functional β-cyclodextrin which engages with GM3 glycolipid *via* a CCI to enable successful delivery of doxorubicin and may contribute to the lactose 'trojan horse' effect for gaining entry into mammalian cells.[17,18] Dendritic and nanoparticle based systems have been synthesized and evaluated for CCIs.[11,16,19] These extremely weak interactions have been measured using solution NMR,[20] interfacial techniques such as Langmuir-Blodget[19] and scanning probe microscopy[21] and also by surface plasmon resonance (SPR).[14] Seeberger and co-workers developed multivalent 4 nm silica glyco nanoparticles to study GM3-Gg3 interactions.[16] Penades and co-workers have used glycan-functional gold nanoparticles with SPR to demonstrate strong CCI multivalent effects.[15] Russel and coworkers used PEG-lactose functional gold particles for the plasmonic detection (red-blue colour change) of CCIs,[22] enable simple and accessible read-outs, which have also found application in biosensing.[10]

A challenge in studying CCIs is that many of these are self-interactions, e.g. lactose-lactose. Therefore, it is desirable to prevent spontaneous interactions between synthetic multivalent systems, by introducing an inducible 'trigger' such that the glycan is presented with temporal, or spacial control to underpin their study. In Nature this is achieved by expression of glycosyltransferases which installs the glycan when required, depending on internal/external cues such as disease state.[23,24] There are many examples of stimuli-responsive polymers,[25] capable of changing their form (e.g. coli-globule transition) in response to redox,[26] light[27] and metal ions.[28] Mastrotto *et al* have used the reversible collapse of poly(*N*-isopropyl acrylamide) to present folate on particle surfaces for cellular delivery using thermal[29] and pH stimuli.[30] Sequential revealing of ligands on liposomes has enabled improved deliver of liposome formulations.[31] Spain and Alexander have used DNA strand displacement for oligonucleotide-specific ligand expression.[32] Won et al demonstrated responsive polymers can provide a reversible steric 'shield' to present glycans at gold nanoparticle surfaces ensuring lectin binding only occurs when the system is activated.[33]

Herein we describe dynamic nanomaterials where the surface expression of glycans can be externally triggered, to induce a carbohydrate-carbohydrate interaction. We show that polymeric gates can effectively block a (shorter) polymer bound glycan and present it at the surface of a gold nanoparticle on demand, and exploit the coupling of gold particle SPRs to monitor the interaction colourmetrically under the control of a small temperature change. By engineering an inducible trigger, these systems will facilitate the study and exploitation of CCIs in biotechnological fields.

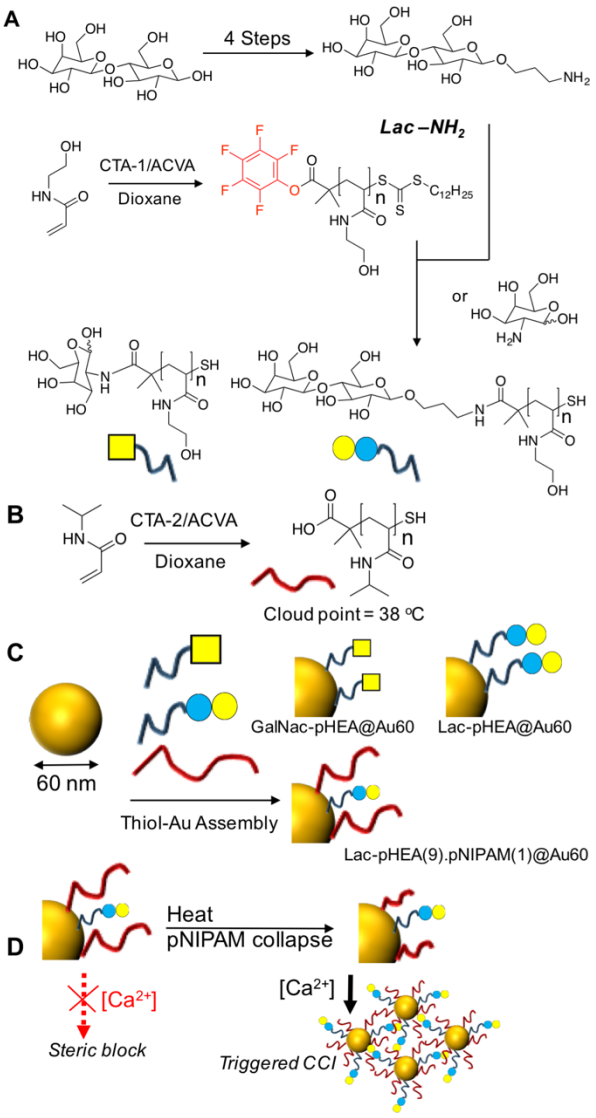

Figure 1. Synthesis of gated glycoparticles. A) Synthesis of glycosylated pHEA; B) Synthesis of pNIPAM; C) Homo-and hetero-genous coating of gold nanoparticles; D) concept of thermo-responsive polymer gate to control expression of lactose at the nanoparticle surface. Initiator = 4,4'-azobis(4-cyanopentanoic acid).

Table 1. Polymer characterization

Polymer	[M]/[CTA]/[I] [mol]	Conv.[(a)] [%]	$M_{n\ Theo}$[(b)] [g mol^{-1}]	$M_{n\ SEC}$[(c)] [g mol^{-1}]	Đ [-]	CP[(d)] [°C]
PFP-pHEA$_{15}$	15/1/0.2	93 %	2100	4800	1.10	-
pNIPAM$_{50}$	50/1/0.2	86 %	5200	7100	1.10	38

(a)^{1}H NMR; [(b)] [M]:[CTA] and conversion; [(c)] Compared to PS standards; [(d)] cloud point determined by turbidimetry at 1.0 mg mL^{-1}.

Our design principle requires a non-responsive polymer bearing a glycan, and a responsive polymer to act as the reversible gate: poly(*N*-hydroxyethyl acrylamide) (pHEA) and poly(*N*-isopropylacrylamide) (pNIPAM) were respectively chosen.[33] pNIPAM was polymerized using CTA-2 2-(dodecylthiocarbonothioylthio)-2-methylpropionic acid). pHEA was polymerized using CTA-1 (pentafluorophenyl 2-(dodecylthiocarbonothioylthio)-2-methylpropionic acid) which enables installation of amino-glycans onto the chain-end by displacement of the PFP group.[34] PFP-pHEA$_{15}$ was functionalized by addition of 2-amino-2-deoxy-D-galactose (GalNH$_2$) or 1-aminopropyl-D-lactose (LacNH$_2$), which was synthesized in 4 steps from lactose (ESI). Addition of the glycans also results in cleavage of the RAFT agent producing a terminal thiol suitable for immobilization onto citrate-stabilized gold nanoparticles. To ensure that the glycan-bearing polymer (pHEA) can be 'hidden' by the responsive polymer (pNIPAM) the targeted degrees of polymerization were 15 and 50 respectively.[33] SEC analysis showed slightly higher molecular weights than NMR for the pHEA and that polymers were well-defined, with Đ <1.1. ^{1}H NMR and IR spectroscopies confirmed installation of the glycan. pNIPAM$_{50}$ had a cloud point of 38 °C at 1 mg mL^{-1}. Once immobilised on the nanoparticle the actual transition temperature will vary,[35] hence a full concentration dependent study on this well-known polymer was not undertaken.[26]

60 nm Gold nanoparticles (Au$_{60}$) were coated with the indicated (Table 2) ratios of each polymer to generate particles bearing either pure glycan coatings, or mixed glycan/responsive polymer coatings, which have been found to give grafting densities ~ 0.3 chains/nm^{-2}.[36] Polymer coating was confirmed by the shift of the SPR$_{MAX}$ peak to longer wavelength and dynamic light scattering showed an increase in diameter from 58 to ~ 70 nm. There was also a corresponding increase in the zeta potential. The particles had a net-negative charge as is widely reported for coating by this method,[32] but the particles (see below) remain stable in buffered saline solutions. pNIPAM containing polymers had cloud points above 50 °C but it is crucial to note that the actual chain collapse occurs below this temperature, essential for the present work.[35]

Table 2. Nanoparticle characterization

Particle	SPR[(a)] [nm]	Diameter[(b)] [nm]	CP[(c)] [°C]	ζ[(d)] [mV]
Au$_{60}$	534	58	-	-41[(e)]
pNIPAM$_{50}$@Au$_{60}$	538	75	59	-15
Lac-pHEA$_{15}$(9) /pNIPAM$_{50}$(1)@Au$_{60}$	538	67	52	-14
Lac-pHEA$_{15}$@Au$_{60}$	537	66	-	-11
GalNAc-pHEA$_{15}$@Au$_{60}$	537	66	-	-9

[(a)] Surface plasmon resonance band; [(b)] determined by DLS; [(c)] determined in water by UV-Vis spectroscopy; [(d)] Conducted in HEPES buffer unless noted; [(e)] Conducted in water. Total gold particle concentration (0.0255 mg mL^{-1})

With this panel of nanoparticles bearing both responsive/non-responsive units and two different glycans to hand, control experiments were undertaken to demonstrate glycan-driven interactions at the particle surface. Lac-pHEA$_{15}$@Au$_{60}$ and GalNAc-pHEA$_{15}$@Au$_{60}$ (i.e. non-responsive coatings) were exposed 0.1 to 100 mM of Ca^{2+}. Ca^{2+} is the primary divalent ion which bridges appropriate glycans to initiate the CCI. Following 30 min incubation Lac-pHEA$_{15}$@Au$_{60}$ showed distinct shifts in its UV-Vis with the SPR$_{MAX}$ decreasing and Abs$_{700}$ increasing, consistent with cross-linking, Figure 2.[36,38] Conversely, addition of Ca^{2+} to GalNAc-pHEA$_{15}$@Au$_{60}$ showed very minor spectral changes with essentially zero aggregation (isotherms in ESI). TEM analysis confirmed these observations (Figure 2E). GalNAc does not undergo self-self CCIs and hence excluded the possibility of non-specific interactions due to changes in the ionic

strength of the buffers. Similar results were obtained using Mn^{2+}, also a divalent cation which can drive CCI (ESI). To further corroborate the link between glycan presentation and aggregation, a lectin-mediated (carbohydrate-protein) interaction was also studied. SBA (soy bean agglutinin) was chosen as it has high affinity for GalNAc but lower affinity for lactose (i.e. opposite response to CCI expected).[39] A serial dilution of SBA was added to both nanoparticles from 10 – 100 nM and UV-Vis spectra recorded (Figure 2C/D). SBA requires calcium to be present in the binding mix, but at concentrations which did not cause CCI aggregation. Lac-$pHEA_{15}$@Au_{60} showed no aggregation but GalNAc-$pHEA_{15}$@Au_{60} underwent strong dose-dependant binding to SBA . These control experiments confirmed the differential presentation of glycans on the nanoparticle surface that the end-group glycosylations provide sufficient density on the particle surface to induce a cluster-glycoside enhancement.

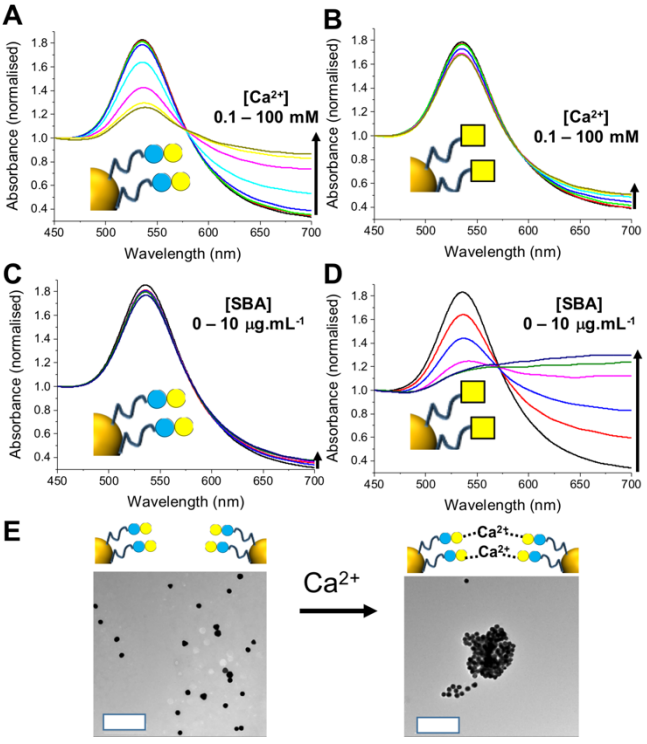

Figure 2. Calcium and lectin triggered aggregation of homogenous glyconanoparticles. A) Lac-$pHEA_{15}$@Au_{60} with Ca^{2+}; B) GalNAc-$pHEA_{15}$@Au_{60} with SBA; C) Lac-$pHEA_{15}$@Au_{60} with SBA; D) GalNAc-$pHEA_{15}$@Au_{60} with SBA; E) TEM analysis of Lac-$pHEA_{15}$@Au_{60} with and without Ca^{2+} Scale bar = 500 nm.

The above data demonstrated the challenge of self-self CCI study; when lactose-functional materials are placed in the biological buffers spontaneous self-aggregation is always going to occur. This complicates detailed studies, especially in cell based assays as the expression of lactose is static, not controllable, but has been reported to drive cell uptake by unknown mechanisms.[17] To evaluate steric gating Lac-$pHEA_{15}$:$pNIPAM_{50}$ ratio 9:1@Au_{60} was monitored for calcium-mediated aggregation at 20 °C. At this temperature, the pNIPAM is fully extended and provides a steric block to CCIs, preventing aggregation even at 100 mM Ca^{2+}, Figure 3A. Time-dependent studies by monitoring Abs_{700} showed only a very slow change and TEM revealed no evidence of aggregation, Figure 3C/D. Hence it can be seen that just 10 mol% of pNIPAM on the particle surface can sterically block CCIs, and is 'gate closed'.

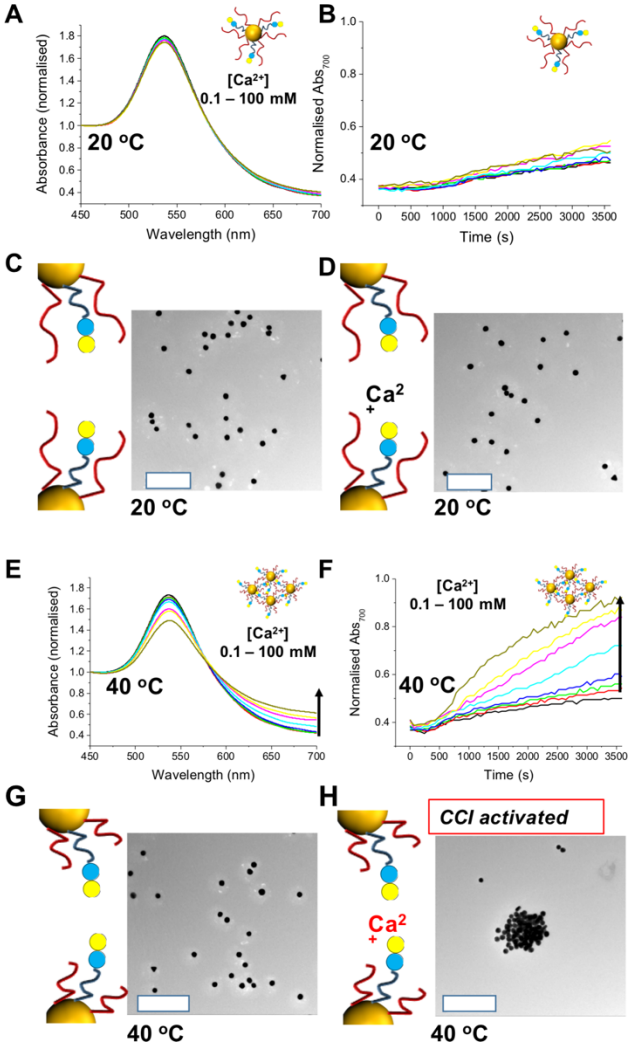

Figure 3. Temperature –controlled gating of lactose expression at Lac-$pHEA_{15}$: $pNIPAM_{50}$ ratio 9:1 @Au_{60} surfaces. Ca^{2+} addition at 20 °C A) full UV-vis and B) time-dependence;. TEM analysis C) without and D) with calcium showing no aggregation. Ca^{2+} addition at 40 °C E) full UV-vis and F) time-dependence;. TEM analysis G) without and H) with calcium showing selective CCI activation. Scale bar = 500 nm.

Identical experiments as above were conducted, but this time at 40 °C which is above the chain collapse temperature of pNIPAM, but below the threshold for them to aggregate (avoiding false positives, see Table 2), Figure 3E/F. Addition of Ca^{2+} lead to a clear increase in Abs_{700} and time-dependent monitoring of these showed rapid aggregation significantly faster and to a greater extent than for at 20 °C. TEM confirmed the formation of aggregates in the presence of $Ca^{2+,}$ but that in the absence of Ca^{2+} (even at 40 °C) there were no non-specific particle-particle interactions. This is the first example of using an external trigger to control a CCI interaction and provides a dynamic tool for studying this area of glycoscience.

To further demonstrate the potential of these responsive nanoparticles, an assay was devised to mimic cell-surface hetero-

CCI interactions; namely lactose-GM-3.[18] A polystyrene plate was modified by physiosorption of GM-3 glycolipid to create a cellular membrane mimic substrate. This was then incubated with both static, and dynamic nanoparticles and binding evaluated by UV-Vis and high-resolution scanning electron microscopy (SEM) after washing, Figure 4A. Due to the low concentration (a monolayer) low UV-Vis signals were obtained but the presence of the SPR peak at ~ 550 nm could be seen when Lac-pHEA@Au_{60} was incubated with calcium at 20 °C, but no SPR peak was seen for the other static particles, Figure 4B. Figure C shows the dynamic particles, Lac-$pHEA_{15}$(9)/$pNIPAM_{50}$(1)@Au_{60}, at both 20 and 40 °C showing nanoparticles were only bound at the higher temperature, when the gate is 'open'. SEM of the GM-3 surfaces corroborated the observations from UV-Vis. Figure 4D/E show that static nanoparticles are captured by GM-3 only for lactose not GalNAc functionality. Figure 4F show the dynamic nanoparticles with 'gate closed' at 20 °C (no binding) and Figure 4G with 'gate open' at 40 °C with significant Lac-GM-3 interactions occurring.

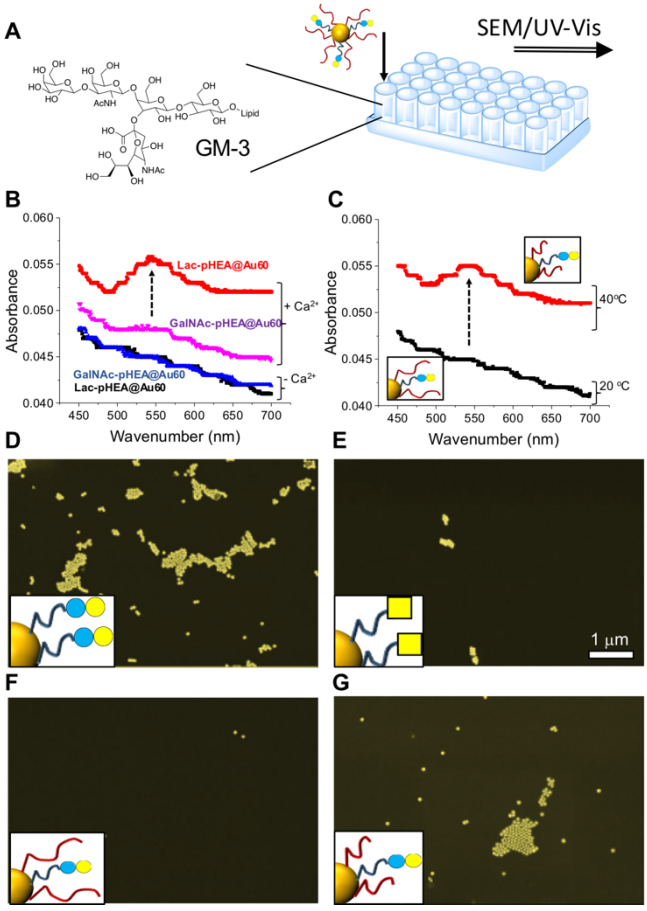

Figure 4. Interactions between glyco nanoparticles and GM-3 surface. A) Experimental concept. B) UV-Vis analysis of GM-3 surface after incubation with 'static' nanoparticles at fixed temperature; C) U-Vis with dynamic nanoparticles + Ca^{2+}. False-colour SEM at GM-3 surfaces of; D) Lac-$pHEA_{15}$@Au_{60} at 20 °C; E) GalNAc-$pHEA_{15}$@Au_{60} 20 °C; F) Lac-$pHEA_{15}$(9)/$pNIPAM_{50}$(1)@Au_{60} at 20 °C; G) Lac-$pHEA_{15}$(9)/$pNIPAM_{50}$(1)@Au_{60} at 40 °C.

Herein we have demonstrated stimuli-responsive, 'triggerable' multivalent glyconanoparticles for the study of carbohydrate-carbohydrate interactions. At the surface of gold nanoparticles non-responsive polymers were used to anchor lactose and a responsive polymer, which can collapse upon application of a thermal stimulus used as a steric 'gate'. By exploiting this trigger, and the unique optical properties of the gold nanoparticle core, it was possible to monitor aggregation due to the lactose-lactose interactions in a label-free manner, and upon application of the external stimulus. The hetero Lac-GM-3 interaction was also probed by this method using a binding assay which mimics a cell-surface interaction, demonstrating selective binding only upon application of the stimulus. This method enables temporal control of when the glycans are expressed on the nanoparticle surface, comparable to enzymatic control in Nature preventing unwanted spontaneous interactions, entirely under the operators control. This will facilitate the study and exploitation of multivalent carbohydrate interactions.

ASSOCIATED CONTENT

Experimental procedures and characterization data plus additional binding experiments are included in the Supporting Information. This material is available free of charge via the Internet at http://pubs.acs.org.

AUTHOR INFORMATION

Corresponding Author

*E-mail: M.I.Gibson@warwick.ac.uk (M. I. Gibson)

Author Contributions

The manuscript was written through contributions of all authors. All authors have given approval to the final version.

ACKNOWLEDGMENT

The University of Warwick is thanked for a Chancellors International Scholarship for SW. MIG holds an ERC starter grant (CRYOMAT 638661). The Electron Microscopy research technology platform and photo-emission facility were supported by Advantage West Midlands and the ERDF.

REFERENCES

(1) Bertozzi, C. R.; Kiessling; L., L. Chemical Glycobiology. *Science (80-.).* **2001**, *291* (5512), 2357–2364.

(2) Dam, T. K.; Fred Brewer, C. Lectins as Pattern Recognition Molecules: The Effects of Epitope Density in Innate Immunity. *Glycobiology* **2009**, *20* (3), 270–279.

(3) Ambrosi, M.; Cameron, N. R.; Davis, B. G. Lectins: Tools for the Molecular Understanding of the Glycocode. *Org. Biomol. Chem.* **2005**, *3* (9), 1593–1608.

(4) Lundquist, J. J.; Toone, E. J. The Cluster Glycoside Effect. *Chem. Rev.* **2002**, *102* (2), 555–578.

(5) Kiessling, L. L.; Grim, J. C. Glycopolymer Probes of Signal Transduction. *Chem. Soc. Rev.* **2013**, *42* (10), 4476–4491.

(6) Kitov, P. I.; Sadowska, J. M.; Mulvey, G.; Armstrong, G. D.; Ling, H.; Pannu, N. S.; Read, R. J.; Bundle, D. R. Shiga-like Toxins Are Neutralized by Tailored Multivalent Carbohydrate Ligands. *Nature* **2000**, *403* (6770), 669–672.

(7) Richards, S.-J.; Jones, M. W.; Hunaban, M.; Haddleton, D. M.; Gibson, M. I. Probing Bacterial-Toxin Inhibition with Synthetic Glycopolymers Prepared by Tandem Post-Polymerization Modification: Role of Linker Length and Carbohydrate Density. *Angew. Chemie - Int. Ed.* **2012**, *51* (31), 7812–7816.

(8) Becer, C. R.; Gibson, M. I.; Geng, J.; Ilyas, R.; Wallis, R.; Mitchell, D. A.; Haddleton, D. M. High-Affinity Glycopolymer Binding to

Human DC-SIGN and Disruption of DC-SIGN Interactions with HIV Envelope Glycoprotein. *J. Am. Chem. Soc.* **2010**, *132* (43), 15130–15132.

(9) Otten, L.; Vlachou, D.; Richards, S.-J.; Gibson, M. I. Glycan Heterogeneity On Gold Nanoparticles Increases Lectin Discrimination Capacity in Label-Free Multiplexed Bioassays. *Analyst* **2016**, *141* (14), 4305–4312.

(10) Marin, M. J.; Rashid, A.; Rejzek, M.; Fairhurst, S. A.; Wharton, S. A.; Martin, S. R.; McCauley, J. W.; Wileman, T.; Field, R. A.; Russell, D. A. Glyconanoparticles for the Plasmonic Detection and Discrimination between Human and Avian Influenza Virus. *Org Biomol Chem* **2013**, *11* (41), 7101–7107.

(11) de la Fuente, J. M.; Penadés, S. Understanding Carbohydrate-Carbohydrate Interactions by Means of Glyconanotechnology. *Glycoconj. J.* **2004**, *21*, 149–163.

(12) Bucior, I.; Scheuring, S.; Engel, A.; Burger, M. M. Carbohydrate-Carbohydrate Interaction Provides Adhesion Force and Specificity for Cellular Recognition. *J. Cell Biol.* **2004**, *165* (4), 529–537.

(13) Vilanova, E.; Santos, G. R. C.; Aquino, R. S.; Valle-Delgado, J. J.; Anselmetti, D.; Fernàndez-Busquets, X.; Mourão, P. A. S. Carbohydrate-Carbohydrate Interactions Mediated by Sulfate Esters and Calcium Provide the Cell Adhesion Required for the Emergence of Early Metazoans. *J. Biol. Chem.* **2016**, *291* (18), 9425–9437.

(14) Haseley, S. R.; Vermeer, H. J.; Kamerling, J. P.; Vliegenthart, J. F. Carbohydrate Self-Recognition Mediates Marine Sponge Cellular Adhesion. *Proc. Natl. Acad. Sci. U. S. A.* **2001**, *98* (16), 9419–9424.

(15) Hernáiz, M. J.; De La Fuente, J. M.; Barrientos, Á. G.; Penadés, S. A Model System Mimicking Glycosphingolipid Clusters to Quantify Carbohydrate Self-Interactions by Surface Plasmon Resonance. *Angew. Chem. Int. Ed.* **2002**, *41* (9), 1554–1557.

(16) Lai, C.-H.; Hütter, J.; Hsu, C.-W.; Tanaka, H.; Varela-Aramburu, S.; De Cola, L.; Lepenies, B.; Seeberger, P. H. Analysis of Carbohydrate–Carbohydrate Interactions Using Sugar-Functionalized Silicon Nanoparticles for Cell Imaging. *Nano Lett.* **2016**, *16* (1), 807–811.

(17) Benito-Alifonso, D.; Tremel, S.; Hou, B.; Lockyear, H.; Mantell, J.; Fermin, D. J.; Verkade, P.; Berry, M.; Galan, M. C. Lactose as A "trojan Horse" for Quantum Dot Cell Transport. *Angew. Chemie - Int. Ed.* **2014**, *53* (3), 810–814.

(18) Murthy, R. V.; Bavireddi, H.; Gade, M.; Kikkeri, R. Exploiting the Lactose-GM3 Interaction for Drug Delivery. *ChemMedChem* **2015**, *10* (5), 792–796.

(19) Seah, N.; Santacroce, P. V.; Basu, A. Probing the Lactose-GM3 Carbohydrate - Carbohydrate Interaction with Glycodendrimers. *Org. Lett.* **2009**, *11* (3), 559–562.

(20) Santos, J. I.; de Souza, A. C.; Cañada, F. J.; Martín-Santamaría, S.; Kamerling, J. P.; Jiménez-Barbero, J. Assessing Carbohydrate-Carbohydrate Interactions by NMR Spectroscopy: The Trisaccharide Epitope from the Marine Sponge Microciona Prolifera. *ChemBioChem* **2009**, *10* (3), 511–519.

(21) Carvalho de Souza, A.; Vliegenthart, J. F. G.; Kamerling, J. P. Gold Nanoparticles Coated with a Pyruvated Trisaccharide Epitope of the Extracellular Proteoglycan of Microciona Prolifera as Potential Tools to Explore Carbohydrate-Mediated Cell Recognition. *Org. Biomol. Chem.* **2008**, *6* (12), 2095.

(22) Reynolds, A. J.; Haines, A. H.; Russell, D. A. Gold Glyconanoparticles for Mimics and Measurement of Metal Ion-Mediated Carbohydrate - Carbohydrate Interactions. *Langmuir* **2006**, *22* (3), 1156–1163.

(23) Pinho, S. S.; Reis, C. A. Glycosylation in Cancer: Mechanisms and Clinical Implications. *Nat Rev Cancer* **2015**, *15* (9), 540–555.

(24) Moremen, K. W.; Tiemeyer, M.; Nairn, A. V. Vertebrate Protein Glycosylation: Diversity, Synthesis and Function. *Nat. Rev. Mol. Cell Biol.* **2012**, *13* (7), 448–462.

(25) Stuart, M. A. C.; Huck, W. T. S.; Genzer, J.; Müller, M.; Ober, C.; Stamm, M.; Sukhorukov, G. B.; Szleifer, I.; Tsukruk, V. V.; Urban, M.; Winnik, F.; Zauscher, S.; Luzinov, I.; Minko, S. Emerging Applications of Stimuli-Responsive Polymer Materials. *Nat. Mater.* **2010**, *9* (2), 101–113.

(26) Phillips, D. J.; Gibson, M. I. Degradable Thermoresponsive Polymers Which Display Redox-Responsive LCST Behaviour. *Chem. Commun.* **2012**, *48* (7), 1054–1056.

(27) Bertrand, O.; Gohy, J.-F. Photo-Responsive Polymers: Synthesis and Applications. *Polym. Chem.* **2016**, *44* (1), 5539–5553.

(28) Phillips, D. J.; Prokes, I.; Davies, G.-L.; Gibson, M. I. Isothermally-Responsive Polymers Triggered by Selective Binding of Fe3+ to Siderophoric Catechol End-Groups. *ACS Macro Lett.* **2014**, *3* (12), 1225–1229.

(29) Mastrotto, F.; Caliceti, P.; Amendola, V.; Bersani, S.; Magnusson, J. P.; Meneghetti, M.; Mantovani, G.; Alexander, C.; Salmaso, S. Polymer Control of Ligand Display on Gold Nanoparticles for Multimodal Switchable Cell Targeting. *Chem. Commun. (Camb).* **2011**, *47* (35), 9846–9848.

(30) Brazzale, C.; Mastrotto, F.; Moody, P.; Watson, P. D.; Balasso, A.; Malfanti, A.; Mantovani, G.; Caliceti, P.; Alexander, C.; Jones, A. T.; Salmaso, S. Control of Targeting Ligand Display by pH-Responsive Polymers on Gold Nanoparticles Mediates Selective Entry into Cancer Cells. *Nanoscale* **2017**, *9* (31), 11137–11147.

(31) R. M. Sawant; J. P. Hurley; S. Salmaso; A. Kale; E. Tolcheva; T. S. Levchenko, and; Torchilin*, V. P. "SMART" Drug Delivery Systems: Double-Targeted pH-Responsive Pharmaceutical Nanocarriers. **2006**.

(32) Magnusson, J. P.; Fernández-Trillo, F.; Sicilia, G.; Spain, S. G.; Alexander, C. Programmed Assembly of polymer–DNA Conjugate Nanoparticles with Optical Readout and Sequence-Specific Activation of Biorecognition. *Nanoscale* **2014**, *6* (4), 2368–2374.

(33) Won, S.; Richards, S.-J.; Walker, M.; Gibson, M. I. Externally Controllable Glycan Presentation on Nanoparticle Surfaces to Modulate Lectin Recognition. *Nanoscale Horiz.* **2017**, *3* (2), 1593–1608.

(34) Richards, S.-J.; Gibson, M. I. Optimization of the Polymer Coating for Glycosylated Gold Nanoparticle Biosensors to Ensure Stability and Rapid Optical Readouts. *ACS Macro Lett.* **2014**, *3* (10), 1004–1008.

(35) Gibson, M. I.; O'Reilly, R. K. To Aggregate, or Not to Aggregate? Considerations in the Design and Application of Polymeric Thermally-Responsive Nanoparticles. *Chem. Soc. Rev.* **2013**, *42* (17), 7204–7213.

(36) Richards, S.-J.; Otten, L.; Gibson, M. I. Glycosylated Gold Nanoparticle Libraries for Label-Free Multiplexed Lectin Biosensing. *J. Mater. Chem. B* **2016**, *4* (18), 3046–3053.

(37) Zhang, Z.; Maji, S.; Antunes, A. B. da F.; De Rycke, R.; Zhang, Q.; Hoogenboom, R.; De Geest, B. G. Salt Plays a Pivotal Role in the Temperature-Responsive Aggregation and Layer-by-Layer Assembly of Polymer-Decorated Gold Nanoparticles. *Chem. Mater.* **2013**, *25* (21), 4297–4303.

(38) Elghanian, R.; Storhoff, J. J.; Mucic, R. C.; Letsinger, R. L.; Mirkin, C. A. Selective Colorimetric Detection of Polynucleotides Based on the Distance-Dependent Optical Properties of Gold Nanoparticles. *Science (80-.).* **1997**, *277* (5329), 1078–1081.

(39) Wu, A. M.; Lisowska, E.; Duk, M.; Yang, Z. Lectins as Tools in Glycoconjugate Research. *Glycoconjugate Journal*. Springer US November 27, 2009, pp 899–913.

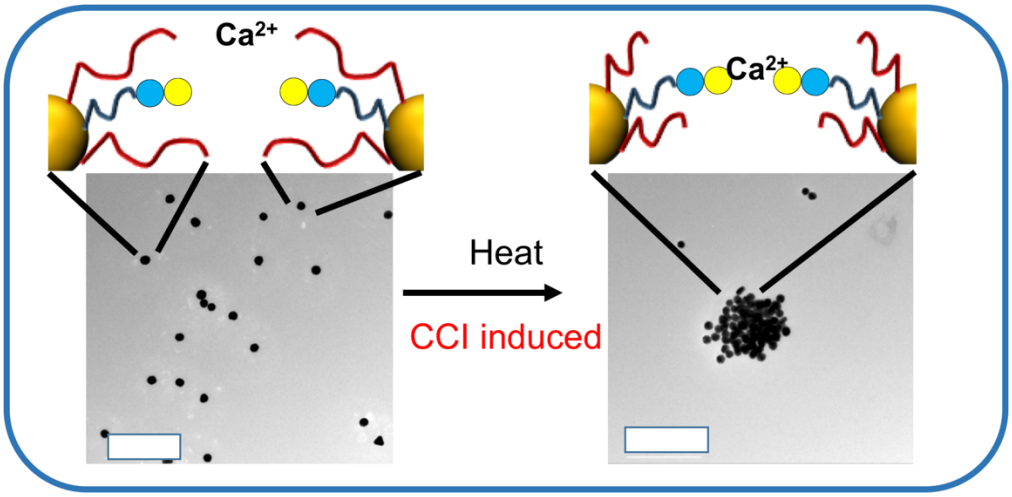
Ca2+
Heat
CCI induced
Ca2+